

In Situ Deposition of Co_9S_8 Nanocrystallite on Its Single-Crystal Flakes at Low Temperatures

Yuanguang Zhang,[1,2] Fan Guo,*[,1] Songming Wan,[1] Weiwei Zheng,[1] and Yiya Peng[1]

[1]Structure Research Laboratory and Department of Chemistry, University of Science & Technology of China, Hefei 230026, P. R. China

[2]Department of Chemistry, Anqing Normal College, Anqing 246011, P. R. China

Received August 16, 2004; E-mail: ygz@mail.ustc.edu.cn

Co_9S_8 hexagonal aggregations were synthesized in hydrazine hydrate ($N_2H_4 \cdot H_2O$) solvent at 150 °C for 12 h using cobalt(II) sulfate hydrate ($CoSO_4 \cdot 7H_2O$) and sodium sulfite (Na_2SO_3) as starting materials through a hydrothermal controlled-reduction method. The as-prepared samples were characterized by X-ray diffraction (XRD), field-emission scanning electron microscopy (FE-SEM), and transmission electron microscopy (TEM), and their magnetic properties were evaluated on a vibrating sample magnetometer (VSM). The results showed the samples were mainly composed of Co_9S_8 hexagonal aggregations with an average diameter of 2.2 μm and a thickness of 200 nm. About 3 nm Co_9S_8 nanocrystallites deposited on its single-crystal flakes. The products exhibited ferromagnetism; the saturation magnetization (M_s) and coercivity (H_c) values of the samples were 80 emu/g and 320 Oe, respectively. The possible formation mechanism of Co_9S_8 hexagonal aggregations is discussed.

There are many phases of cobalt sulfides, such as CoS, Co_3S_4, CoS_2, and Co_9S_8. Among them, Co_9S_8 and CoS_2 have attracted attention concerning their properties for a long time.[1] Co_9S_8 is of importance in hydrodesulfurization catalysts and magnetic devices.[2] Usually, cobalt sulfides are synthesized using solid state reactions between stoichiometric amounts of the constituent elements in evacuated silica tubes in the temperature range 500–1200 °C,[3,4] but a higher firing temperature process will lead to a larger particle size and inhomogeneity, and it is difficult to obtain single phases of these sulfides.

Cobalt sulfides could also be prepared by the reaction of cobalt or cobalt monoxide with hydrogen sulfide.[5,6] Although many routes have been shown to prepare cobalt sulfides, the conditions for obtaining Co_9S_8 are not very specific. To our knowledge, a mid-temperature synthesis route of Co_9S_8 has been reported involving the treatment of anhydrous cobalt sulfate salt in a flowing gas of hydrogen sulfide and hydrogen at 525 °C,[7] but there are few reports about the formation of Co_9S_8 by a low-temperature hydrothermal method.[8] Hydrothermal synthesis is one of the promising solution chemical methods, by which the particle size and phase homogeneity can be well controlled.[9,10] Here, we report on a low-temperature facile synthesis of Co_9S_8 hexagonal aggregations using low-cost sodium sulfite (Na_2SO_3) to supply a sulfur source and hydrazine hydrate ($N_2H_4 \cdot H_2O$) as a reducing and complexing agent through a hydrothermal controlled-reduction method.

Experimental

All analytical grade reagents were purchased from Shanghai Chemical Company and used without further purification. In a typical procedure, cobalt(II) sulfate hydrate ($CoSO_4 \cdot 7H_2O$, 0.879 g) was dissolved in 20 mL of distilled water; then, sodium sulfite (Na_2SO_3, 0.326 g) was added under stirring, followed by adding 15 mL of hydrazine hydrate ($N_2H_4 \cdot H_2O$, 80 vol %) to form a mixture. The mixture was strongly stirred for 30 min at room temperature, and then transferred into a Teflon-lined stainless-steel autoclave with a capacity of 60 mL, which was filled with distilled water up to 80% of the total volume. The autoclave was sealed and maintained at 150 °C for 12 h. The system was then allowed to cool to room temperature naturally. Black products were collected by filtration, washed with distilled water and absolute ethanol several times. The final products were dried under a vacuum at 60 °C for 3 h.

The X-ray powder diffraction (XRD) pattern was recorded on a Japan Rigaku D/max-γA X-ray diffractometer using Cu Kα radiation ($\lambda = 1.5418$ Å). A field-emission scanning electron microscope (FE-SEM) measurement was carried out with a field-emission microscope (JEOL, 7500B) operated at 10 kV. Transmission electron microscope (TEM) images were taken using a Hitachi Model H-800 transmission electron microscope operated at 200 kV. The magnetization loop was measured at room temperature using a BHV-55 vibrating sample magnetometer (VSM).

Results and Discussion

Figure 1 shows a typical XRD pattern of the as-prepared samples. All of the diffraction peaks in Fig. 1 can be well indexed to a pure cubic phase of Co_9S_8 [space group: *Fm*3*m* (225)] with a lattice constant of $a = 9.926$ Å, which is in good agreement with the literature value of $a = 9.928$ Å (JCPDS cards, No. 73-1442). No characteristic peaks of impurity phases, such as CoO and other cobalt sulfides, are observed. The average crystalline size of the samples, estimated by the Scherrer equation with a shape factor of 0.89 applied, is about 3 nm. In addition, the changes of the intensity ratio in the present case imply that the as-prepared samples may have orientation.

Figure 2 shows FE-SEM images of the as-prepared samples.

Published on the web February 11, 2005; DOI 10.1246/bcsj.78.277

The pictures indicate that the products display hexagonal platelets with an average diameter of 2.2 μm and a thickness of 200 nm, respectively. TEM observation shows that the samples are mainly composed of many Co_9S_8 hexagonal aggregations, and there are a number of small Co_9S_8 particles on hexagonal aggregations [Figs. 3a, 3b]. The hexagonal aggregations are about 2.2 μm in diameter and 200 nm in thickness, respectively, which is consistent with FE-SEM results. In Fig. 3c, the corresponding electron diffraction (ED) pattern was taken from a single hexagonal aggregation. In the pattern, there are obvious polycrystalline diffraction rings, which from the innermost to the outmost correspond to the (111), (311), (222), (331), (422), (511), (440), and (622) diffraction of cubic Co_9S_8, and the *d* values deduced from this figure agree well with that of the XRD pattern. It can be considered that the prepared hexagonal aggregations consist of Co_9S_8 nanocrystallites.

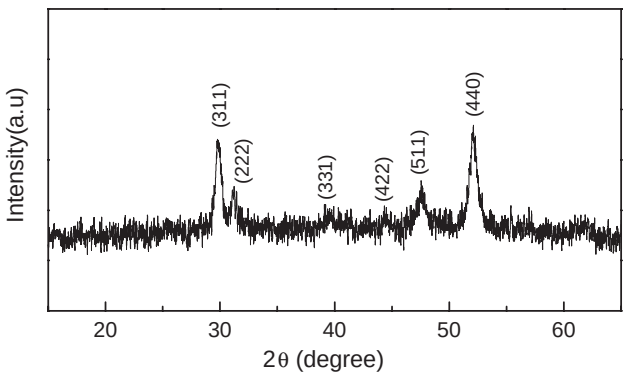

Fig. 1. XRD pattern of the as-prepared samples.

During the formation of Co_9S_8 products, we make use of redox reaction to control S^{2-} concentration, which can be shown as follows:

$$2\ SO_3^{2-} + 3\ N_2H_4 \rightarrow 2\ S^{2-} + 3\ N_2 + 6\ H_2O. \qquad (1)$$

Based on the values of E°, the standard potential of the SO_3^{2-}/S^{2-} couple in alkaline solutions is -0.61 V. The potential for the redox couple N_2H_4/N_2 (-1.16 V) is negative enough for the SO_3^{2-} reduction to S^{2-}. When $N_2H_4 \cdot H_2O$ is added, the $[Co(N_2H_4)_m]^{2+}$ complex will be formed.[11,12] Newly produced S^{2-} will react with the $[Co(N_2H_4)_m]^{2+}$ complex, and then form the Co_9S_8 products. No other phases are produced; one possible reason is that the formation of $[Co(N_2H_4)_m]^{2+}$ leads $E_{Co^{2+}/Co}$ to decrease greatly. It is difficult to produce

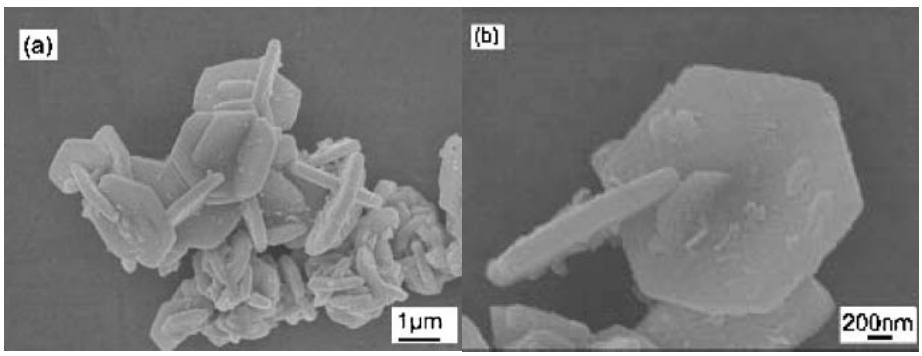

Fig. 2. (a) FE-SEM images of the as-prepared samples. (b) An enlargement of selected area of the as-prepared samples.

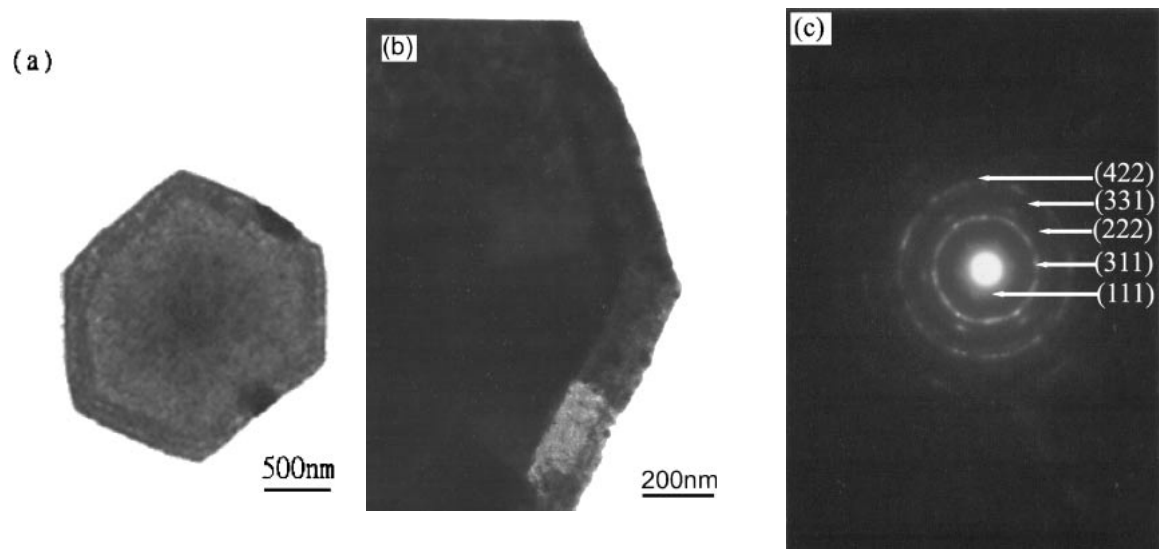

Fig. 3. TEM images of the as-prepared samples. (a) a single hexagonal aggregation, (b) selected area of a single hexagonal aggregation, (c) ED pattern of a single hexagonal aggregation.

elemental cobalt and other cobalt sulfides; another reason is that Co_9S_8 has a large stability, which results mainly from the formation of a structure-induced pseudogap at the Fermi energy,[13] and the larger heat of formation compared to that of the other cobalt sulfides.[14]

During the initial stage of reduction, the nucleation rate of Co_9S_8 in the autoclave is slow because of the lower concentration of S^{2-} anions and the crystallinity of Co_9S_8 is good. Thus, some of the Co_9S_8 single crystallite would be gradually formed in the system. The as-formed Co_9S_8 single crystalline may be grown gradually to form various layer-structure single-crystal flakes, such as a monolayer (Fig. 4a), a bi-layer (Fig. 4b), or multilayers (Fig. 4c). Using TEM, we observed the structure of a monolayer Co_9S_8 single-crystal flake (Fig. 4a), and found that it is highly sensitive to beam exposure. Its structure can be destroyed after several seconds of intensive electron beam irradiation. Figure 4d shows a corresponding electron diffraction (ED) pattern of a monolayer Co_9S_8 single-crystal flake, displaying single-crystal electron-diffraction spots and polycrystalline electron-diffraction rings. The single-crystal electron diffraction spots are formed when a monolayer Co_9S_8 single-crystal flake is exposed to intensive electron-beam irradiation. After several seconds, polycrystalline electron diffraction rings appear, which can be indexed to a cubic Co_9S_8 phase. From the single-crystal electron diffraction spots, we can deduce that the crystal belt axis of the Co_9S_8 single-crystal flakes is $[\bar{1}11]$. A further analysis of the electron diffraction about Co_9S_8 single-crystal flakes will be difficult because of its beam sensitivity.

With Co_9S_8 single-crystal flakes formation, we deduced that the reaction (1) rate may become fast for a period of time, and more S^{2-} anions would be produced during this stage. Therefore, because the Co_9S_8 nucleation rate is expedited, it is easy to form polycrystalline Co_9S_8. On the other hand, the possibility of Co_9S_8 nucleation on the surface of hexagonal Co_9S_8 single-crystal flakes is larger than that in the solution, because the Co_9S_8 nucleation energy on the surface of hexagonal Co_9S_8 single-crystal flakes is lower than that in the solution. Therefore, many Co_9S_8 polycrystallites will be formed on the surface of hexagonal Co_9S_8 single-crystal flakes, forming Co_9S_8 hexagonal aggregations.

The above process, outlined in Fig. 5 for the formation of Co_9S_8 hexagonal aggregations, can be divided into three main steps: (1) the formation of hexagonal Co_9S_8 single-crystal

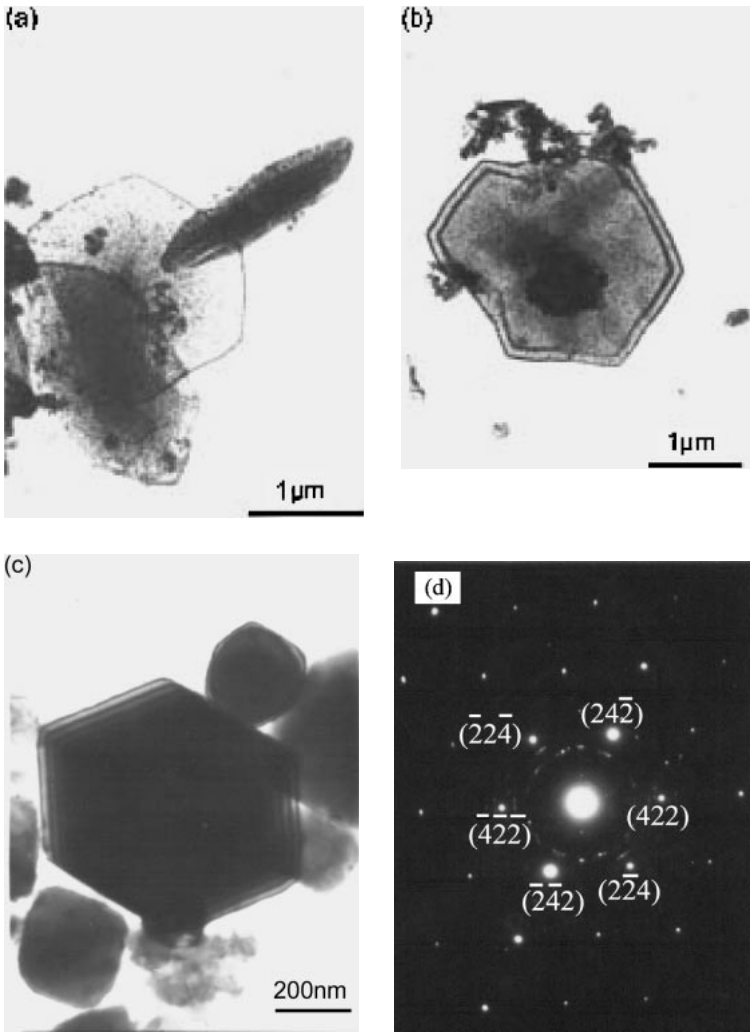

Fig. 4. TEM images of the as-prepared Co_9S_8 single-crystal flakes (a) monolayer, (b) bi-layer, (c) multilayer, (d) ED pattern of a monolayer Co_9S_8 single-crystal flake.

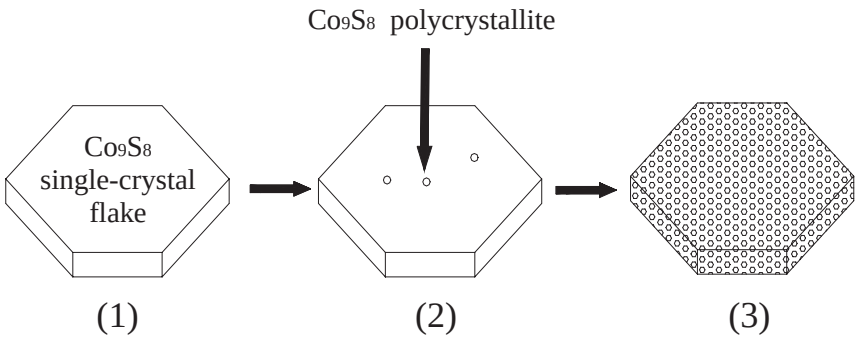

Fig. 5. The whole process presentation of Co_9S_8 hexagonal aggregations: (a) hexagonal Co_9S_8 single-crystal flake, (b) the nucleation on the surface of hexagonal Co_9S_8 single-crystal flake, (c) Co_9S_8 hexagonal aggregations.

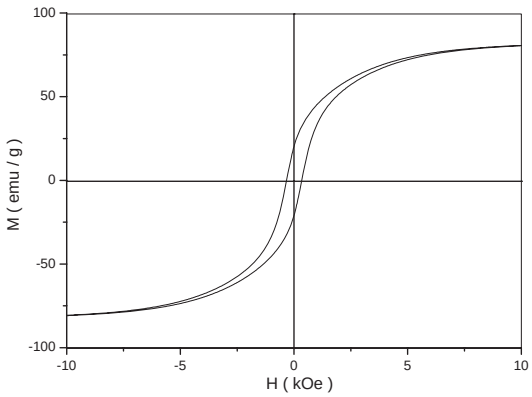

Fig. 6. The room temperature M–H hysteresis loop of the products with an external magnetic field applied.

flakes; (2) Co_9S_8 crystalline nucleation formation on the surface of hexagonal Co_9S_8 single-crystal flakes; and (3) the formation of Co_9S_8 hexagonal aggregations.

Figure 6 shows the room-temperature M–H hysteresis loop of the products with an applied external magnetic field. The saturation magnetization value (M_s) for samples with an external magnetic field is 80 emu/g, and the coercivity value (H_c) for the samples is 320 Oe. It can therefore be deduced that the Co_9S_8 products exhibit ferromagnetism, which belong to soft magnetic materials because of the lower coercivity value.

Conclusion

Co_9S_8 hexagonal aggregations were prepared by reactions between cobalt(II) sulfate hydrate ($CoSO_4 \cdot 7H_2O$) and sodium sulfite (Na_2SO_3) through a hydrazine hydrate ($N_2H_4 \cdot H_2O$) thermal process at 150 °C for 12 h. The XRD pattern indicated that the products were cubic Co_9S_8 single phase. FE-SEM and TEM images showed that the as-prepared samples were mainly composed of Co_9S_8 hexagonal aggregations consisting of Co_9S_8 nanocrystalline with an average size of 3 nm. The prepared Co_9S_8 hexagonal aggregations were about 2.2 μm in diameter and 200 nm in thickness. The magnetic measurements indicated that the products had ferromagnetism. The prepared sample suggests many possible applications in magnetic devices and catalysis.

We would like to thank Prof. Q. W. Chen for valuable discussions. This work was supported by the National Natural Science Foundation of China.

References

1 A. Wold and K. Dwight, *J. Solid State Chem.*, **96**, 53 (1992).
2 T. A. Pecoraro and R. R. Chianelli, *J. Catal.*, **67**, 430 (1981).
3 B. Morris, V. Johnson, and A. Wold, *J. Phys. Chem. Solids*, **28**, 1565 (1967).
4 L. F. Schneemeyer and M. J. Sienko, *Inorg. Chem.*, **19**, 789 (1980).
5 J. C. Colson, *C. R. Acad. Sci.*, **259**, 3261 (1964).
6 P. Barret, J. C. Colson, and D. Delafosse, *C. R. Acad. Sci., Ser. C*, **262**, 83 (1966).
7 D. M. Pasquariello, R. Kershaw, J. D. Passaretti, K. Dwight, and A. Wold, *Inorg. Chem.*, **23**, 872 (1984).
8 J. H. Zhan, X. G. Yang, Y. Xie, D. W. Wang, Y. T. Qian, and X. M. Liu, *J. Mater. Res.*, **14**, 4418 (1999).
9 Y. T. Qian, Y. Su, Y. Xie, Q. W. Chen, and Z. Y. Chen, *Mater. Res. Bull.*, **30**, 401 (1995).
10 Y. T. Qian, Q. W. Chen, Z. Y. Chen, C. G. Fan, and G. E. Zhou, *J. Mater. Chem.*, **3**, 203 (1993).
11 F. Guo, H. G. Zheng, Z. P. Yang, and Y. T. Qian, *Mater. Lett.*, **56**, 906 (2002).
12 Y. C. Zhu, H. G. Zheng, Q. Yang, A. L. Pan, Z. P. Yang, and Y. T. Qian, *J. Cryst. Growth*, **260**, 427 (2004).
13 P. Raybaud, J. Hafner, G. Kresse, and H. Toulhoat, *J. Phys.: Condens. Matter*, **9**, 11107 (1997).
14 H. R. Chauke, D. Nguyen-Manh, P. E. Ngoepe, D. G. Pettifor, and S. G. Fries, *Phys. Rev.*, **B66**, 155105 (2002).